Crystal structure and negative thermal expansion of solid solution $Y_2W_{3-x}Mo_xO_{12}$

J. Peng · M. M. Wu · F. L. Guo · S. B. Han ·
Y. T. Liu · D. F. Chen · X. H. Zhao ·
Z. Hu

Abstract A new series of solid solutions $Y_2W_{3-x}Mo_xO_{12}$ ($0.5 \leq x \leq 2.5$) were successfully synthesized by the solid state method. Their crystal structure and negative thermal expansion properties were studied using high-temperature X-ray powder diffraction and the Rietveld method. All samples of rare earth tungstates and molybdates were found to crystallize in the same orthorhombic structure with space group *Pnca*, and show the negative thermal expansion phenomena related to transverse vibration of bridging oxygen atoms in the structure. Thermal expansion coefficients (TEC) of $Y_2W_{3-x}Mo_xO_{12}$ were determined as -16.2×10^{-6} K^{-1} for $x = 0.5$ and -16.5×10^{-6} K^{-1} for $x = 2.5$ in the identical temperature range of 200–800 °C. High-temperature XRD data and bond length analysis suggest that the difference between W–O and Mo–O bond is responsible for the change of TECs after the element substitution in this series of solid solutions.

J. Peng
Experimental Physics Center, Institute of High Energy Physics, CAS, Beijing 100049, China

J. Peng (✉) · Z. Hu
College of Chemistry and Chemical Engineering, Graduate University of the Chinese Academy of Sciences, Beijing 100049, China
e-mail: pengjie@mails.gucas.ac.cn

M. M. Wu · S. B. Han · Y. T. Liu · D. F. Chen
China Institute of Atomic Energy, Beijing 102413, China

F. L. Guo · X. H. Zhao
College of Chemistry, Beijing Normal University, Beijing 100875, China

Introduction

Negative thermal expansion (NTE) was reported in a large family of tungstates and molybdates with the general formula $A_2M_3O_{12}$, where A could be Sc, Y, and lanthanide rare earth elements Ho, Er, Tm, Yb, and Lu [1–10]. NTE materials are widely used for controlling the effective thermal expansion coefficient of composites. This type of compounds crystallizes in space group *Pnca*. Its structure consists of a corner-sharing network of AO_6 octahedra and $W(Mo)O_4$ tetrahedra. The AO_6 octahedra shares corners with six $W(Mo)O_4$ tetrahedra while $W(Mo)O_4$ tetrahedra shares corners with four AO_6 octahedra [1, 3, 4, 8, 9], i.e., each oxygen atom is two coordinated with one +3 cation and one +6 W/Mo cation. The mechanism of their NTE has been explained in terms of transverse vibration of the bridging oxygen atom between the two rigid polyhedra [1]. It has been suggested by Forster et al. that magnitude of NTE in this family is related to cation size. Larger cations expand the octahedra, reducing oxygen–oxygen repulsions within the polyhedra. This facilitates polyhedra shape changes necessary for the rocking motions required by NTE [10].

All of these $A_2M_3O_{12}$ phases are hygroscopic at room temperature [5, 6, 8–10]. Since Yttrium has almost the biggest ionic radius (0.90 Å) contrasted to lanthanide rare earth elements [11, 12], we chose $Y_2W_{3-x}Mo_xO_{12}$ ($0.0 \leq x \leq 3.0$) series as our study expecting these are the compounds within the $Sc_2W_3O_{12}$ type structure [9, 13]. The pure phases of $Y_2W_3O_{12}$ and $Y_2Mo_3O_{12}$ have different TEC of -22.0×10^{-6} and -19.2×10^{-6} K^{-1}, respectively [8, 9], in despite of the fact that they have the same crystal structure and almost the same ionic radii for W^{3+} (0.42 Å) and Mo^{3+} (0.41 Å) [11]. Also, little study has previously been done on substitution of position M in the

$A_2M_3O_{12}$-type compounds except the $Al_2Mo_{3-x}W_xO_{12}$ series, where it was found that substitution of W for Mo could affect structural and thermal expansion properties of the unsubstituted phases [14, 15]. It is thus of interest to explore changes in the structure and thermal expansion properties of solid solution $Y_2W_{3-x}Mo_xO_{12}$ ($0.0 \leq x \leq 3.0$). Here we report such results mentioned above.

Experimental

$Y_2W_{3-x}Mo_xO_{12}$ ($0.5 \leq x \leq 2.5$) solid solutions were synthesized through the conventional solid state route from corresponding oxides Y_2O_3 (purity 99.5%), MoO_3 (purity $\geq$99.5%) and WO_3 (purity $\geq$99.0%). The reactants were preheated at 500 °C for 4 h before thorough mixing in stoichiometric proportion, then calcined at 700 °C for 12 h, followed by sintering at 1000 °C for 24 h then 1100 °C for 24 h, with one regrinding in between. All samples were slowly cooled to room temperature in furnace.

Room temperature X-ray diffraction (XRD) data were collected on a MSAL-XD2 powder diffractometer with Cu K_α radiation in 2θ range from 10° to 70° by step scanning. High-temperature powder XRD data were collected on a Panalytical X'pert Pro MPD with an Anton Parr high-temperature attachment also using Cu K_α ($\lambda = 1.54056$ Å, 40 kV, 40 mA). A platinum heater was used as sample stage. The temperature was controlled at an accuracy of 1 °C by an Eurotherm temperature programmer. The heating speed was 30 °C min^{-1} and data were collected after temperature was kept constant for 5 min. Rietveld refinements of the diffraction data were performed using the program suite Fullprof [16].

Results and discussion

Room temperature XRD data and structure

Phase identification of the samples with different Mo content was performed through XRD at room temperature. Figure 1 shows the XRD data of $Y_2W_{3-x}Mo_xO_{12}$ ($x = 0.5$, 1.0, 1.5, 2.0, and 2.5) from 10° to 35° to show changes in diffraction patterns. Rough Rietveld analyses of the XRD data indicate that all samples were single phase but hygroscopic and crystallize in orthorhombic form but for $x = 1.5$, which was judged from peak splitting and confirmed as a mixture of $Y_2W_3O_{12}$ and $Y_2Mo_3O_{12}$ by Rietveld refinement. From Fig. 1 it is found the crystal structure changes much with higher level of Mo substitution, including peak shifts and intensity changes. All these changes result from variation of the cell parameters and shifts in atom displacements within the unit cell, even the
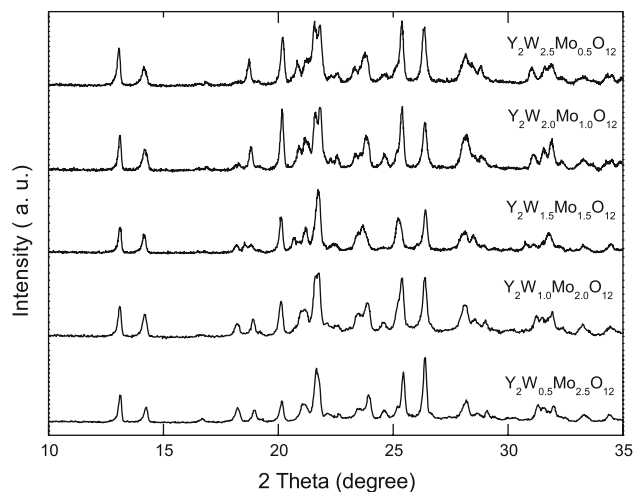

Fig. 1 XRD patterns of solid solution $Y_2W_{3-x}Mo_xO_{12}$ ($0.5 \leq x \leq 2.5$) at room temperature

Table 1 Lattice parameters of $Y_2W_{3-x}Mo_xO_{12}$ ($x = 0.5$, 1.0, 1.5, 2.0, and 2.5) at room temperature

Compound	a (Å)	b (Å)	c (Å)	V (Å^3)	Ref.
$Y_2W_3O_{12}$	10.074 (2)	13.952 (2)	9.990 (2)	1404.4 (3)	[8]
$Y_2W_{2.5}Mo_{0.5}O_{12}$	9.743 (2)	13.981 (3)	9.701 (2)	1321.4 (5)	
$Y_2W_{2.0}Mo_{1.0}O_{12}$	10.0517 (7)	13.529 (1)	9.8017 (8)	1332.9 (2)	
$Y_2Mo_3O_{12}$ ($x = 1.5$)	10.1694 (7)	13.4596 (8)	9.7331 (7)	1332.2 (1)	
$Y_2W_3O_{12}$ ($x = 1.5$)	9.9684 (7)	13.7635 (8)	9.8708 (7)	1354.3 (2)	
$Y_2W_{1.0}Mo_{2.0}O_{12}$	10.017 (1)	13.525 (2)	9.839 (1)	1333.0 (3)	
$Y_2W_{0.5}Mo_{2.5}O_{12}$	9.9849 (9)	13.522 (1)	9.835 (1)	1328.6 (2)	
$Y_2Mo_3O_{12}$	10.044 (3)	13.889 (4)	9.954 (2)	1388.6 (6)	[9]

presence of water molecules. Also, it was verified that these Y series compounds are more hygroscopic than other heavy rare earth elements lanthanides. Rietveld refinements also indicate significant changes appear in these compounds. For Yttrium has almost the biggest ionic radius contrasted with heavy rare earth, and then its molybdate and tungstate correspondingly have most open crystal structure. Therefore inside the crystal cell, there exists much vacant space for water molecules to enter.

Table 1 gives rough refined results of lattice parameters of $Y_2W_{3-x}Mo_xO_{12}$ ($0.5 \leq x \leq 2.5$) solid solutions at room temperature, for comparison, cell parameters of unhydrated $Y_2W_3O_{12}$ and $Y_2Mo_3O_{12}$ are included [8, 9]. As mentioned above, lattice parameters a, b, c, and unit cell volume V change with no obvious trend though the ionic radius of Mo^{3+} is smaller than that of W^{3+}. The dependence of lattice parameters on molybdenum content does not follow the Vegard's law [17, 18], indirectly confirming the presence of water. For as supposed, lattice parameters and unit cell volume will decrease with the increasing molybdenum content. Comparing with the unhydrated phase [8, 9], cell parameters a, b, c, and unit volume V of $Y_2W_3O_{12}$ phase

decrease, which was probably due to the presence of water molecules proposed by Duan et al. [19], where the authors found hydrated ZrW_2O_8 is smaller than unhydrated phase. For $Y_2Mo_3O_{12}$, other than the cell parameter a which increases from 10.044(3) to 10.1694(7) Å, both b and c decrease, and the unit cell volume decreases from 1388.6(1) to 1332.2(1) Å^3. There is no certain relation between the presence of water molecules and individual cell parameter a, b and c, but cell volume V. It is then calculated that after getting rid of water molecules, the cell volume increase 3.7 and 4.2% for $Y_2W_3O_{12}$ and $Y_2Mo_3O_{12}$, respectively. Sumithra et al. [5] found that the cell volume of the hydrated pattern is 7% smaller than the unhydrated cell volume for $Y_2W_3O_{12}$. According to the variation of cell volume with and without water molecules, it could be concluded that the $Y_2Mo_3O_{12}$ is easier to absorb water molecules than $Y_2W_3O_{12}$. Comparing the cell parameters of $Y_2W_{1.0}Mo_{2.0}O_{12}$ with those of $Y_2W_{0.5}Mo_{2.5}O_{12}$, it was found that a, b, c, and V all decrease when W is substituted by smaller Mo atoms. This observation is understood as a consequence of Mo occupying W positions in the crystal lattice, obeying the Vegard's law. Because of the difference in ionic radius, the lattice becomes smaller with Mo substitution.

High-temperature XRD and negative thermal expansion

To study the effects of M site cation substitution on thermal expansion properties, high-temperature X-ray powder diffraction data were collected for $Y_2W_{3-x}Mo_xO_{12}$ ($x = 0.5$, 2.5) at 200, 400, 600, and 800 °C. As an example, the observed and calculated XRD pattern of $Y_2W_{0.5}Mo_{2.5}O_{12}$ at 800 °C and their difference is illustrated in Fig. 2. From figure match and R value, it can be judged that the refinement result is very well. Also none of the high-temperature XRD patterns of $Y_2W_{0.5}Mo_{2.5}O_{12}$ showed any substantial change in the experiment temperature range of 200–800 °C (Fig. 3), which indicates that the compound structures keep unchanged and no phase transition was observed for the selected study range. Contrasting with room temperature diffraction profile (Fig. 1), much difference between peak intensity and profile can be found. However, almost all the peaks shift toward high angle range with increasing temperature, for example, peaks (111) (131) (123), that means under the same X-ray wavelength (λ), scattering angle (θ) increases, to obey the Bragg equation ($2d \sin\theta = \lambda$), the distance between different crystal planes (d) must decrease, then the crystal cell shrink and negative thermal expansion behavior appears with rising temperature. Cell parameters and unit cell volume values at different temperatures are listed in Table 2. Due to the complication of water molecules staying in samples at low temperature, only the data from
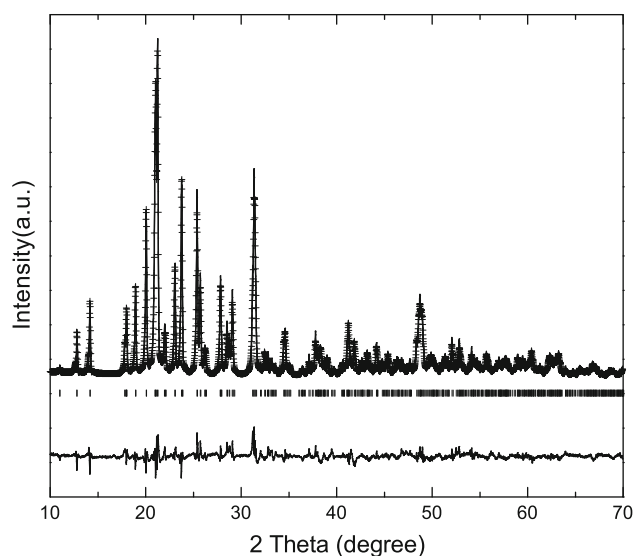

Fig. 2 Results of the Rietveld analysis of the XRD patterns of $Y_2W_{0.5}Mo_{2.5}O_{12}$ at 800 °C ($R_p = 5.97\%$, $R_{wp} = 7.63\%$, and $R_{exp} = 2.02\%$). The *solid line* represents the raw data. The *plus signs* represent the calculated profile. *Vertical bars* indicate the position of Bragg peaks for this phase. The lowest curve is the difference between the observed and calculated patterns
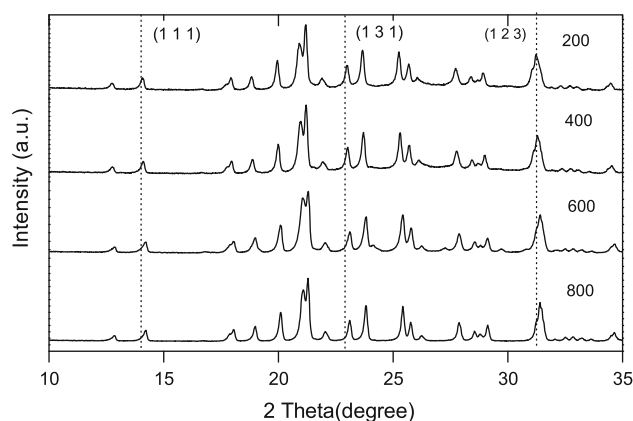

Fig. 3 XRD patterns of $Y_2W_{2.5}Mo_{0.5}O_{12}$ at 200, 400, 600, and 800 °C

Table 2 Crystallographic data of $Y_2W_{3-x}Mo_xO_{12}$ ($x = 0.5$, 2.5) solid solutions at 200, 400, 600, and 800 °C

T (°C)	a (Å)	b (Å)	c (Å)	V (Å^3)
200	10.0316 (9)	13.899 (1)	9.9454 (9)	1386.7 (2)
400	10.0099 (9)	13.894 (1)	9.9314 (9)	1381.3 (2)
600	9.9934 (6)	13.8951 (8)	9.9226 (6)	1377.8 (1)
800	9.9799 (3)	13.8846 (4)	9.9096 (3)	1373.2 (1)
200	10.0175 (9)	13.875 (1)	9.9352 (9)	1380.9 (2)
400	9.9963 (9)	13.871 (1)	9.9207 (9)	1375.6 (2)
600	9.9779 (6)	13.8659 (8)	9.9090 (6)	1371.0 (1)
800	9.9692 (3)	13.8592 (5)	9.8959 (3)	1367.3 (1)

Table 3 The axial and volume thermal expansion coefficients of solid solutions from 200 to 800 °C

Compounds	$\alpha_a \times 10^{-6}$ °C^{-1}	$\alpha_b \times 10^{-6}$ °C^{-1}	$\alpha_c \times 10^{-6}$ °C^{-1}	$\alpha_v \times 10^{-6}$ °C^{-1}	Ref.
$Y_2W_{2.5}Mo_{0.5}O_{12}$	−8.57	−1.73	−6.00	−5.42	
$Y_2W_{0.5}Mo_{2.5}O_{12}$	−8.04	−1.91	−6.58	−5.49	
$Y_2W_3O_{12}$	−9.78	−5.13	−6.68	−7.34	[8]
$Y_2Mo_3O_{12}$	−6.01	−6.25	−7.06	−6.39	[9]

200 to 800 °C are considered. It is seen from Table 2 that cell parameters a, b, c, and unit volumes of $Y_2W_{3-x}Mo_xO_{12}$ ($x = 0.5, 2.5$) decrease with increasing temperature in the whole experiment range, showing strong NTE behavior.

The thermal expansion coefficients can be expressed by the following equations [20]: $\alpha_l = \frac{l_2 - l_1}{l_1}\left(\frac{1}{T_2 - T_1}\right)$ and $\alpha_v = \frac{V_2 - V_1}{3V_1}\left(\frac{1}{T_2 - T_1}\right)$.

where α_l and α_v denote axial and linear volume TEC. l denotes one of the cell parameters a, b, c, while V is the unit cell volume. Because no linear relationships were observed for most of the cell parameters, the average axial and volume TECs are calculated and listed in Table 3, the TECs of unsubstituted phase $Y_2W_3O_{12}$ and $Y_2Mo_3O_{12}$ in the same temperature range 200–800 °C are also tabulated for comparison. From Table 3, it can be seen that for $x = 0.5$, that is Mo was used to replace W, the TECs of α_a, α_b, α_c change from −9.78 to −8.57 × 10^{-6} °C^{-1}, −5.13 to −1.73 × 10^{-6} °C^{-1}, −6.68 to −6.00 × 10^{-6} °C^{-1}, respectively. Therefore, substitution makes the thermal expansion of all axes less negative, leads to the α_v changes from −7.34 to −5.42 × 10^{-6} °C^{-1}. For $x = 2.5$, substitution of W for Mo has almost same effects on the crystal axes, which makes the TEC of α_a change from −6.01 to −8.04 × 10^{-6} °C^{-1}, more negative than before, while axis b and c show less negative, TECs change from −6.25 to −1.91 × 10^{-6} °C^{-1}, −7.06 to −6.58 × 10^{-6} °C^{-1} resulting in the α_v changes from −6.39 to −5.49 × 10^{-6} °C^{-1}. Comparing with the unsubstituted phases, substitution of Mo for W makes α_v decrease 26.2%; substitution of W for Mo makes α_v decrease 14.1%. It is concluded that different substitution elements have different effect on the NTE. With the same substitution content, Mo plays more important roles than W does. The results imply that substitution is a good method to adjust TEC of material, or, in other words, it is possible to obtain materials with desired TEC by adjusting substitution elements and content.

Thermal expansion is usually considered as an effect of anharmonic interatomic potential, with increasing temperature causing thermal expansion of chemical bonds, which in turn leads to expansion of crystal lattice. Evans et al. [1] proposed that negative thermal expansion of the $Y_2(WO_4)_{3-}$-like structure results from transverse vibrations

Table 4 The non-bond distance (Å) and its average of $Y_2W_{3-x}Mo_xO_{12}$ ($x = 0.5, 2.5$) from 200 to 800 °C

	200 °C	400 °C	600 °C	800 °C
Er–W (Mo)	3.893 (13)	3.874 (13)	3.876 (8)	3.895 (5)
	3.903 (15)	3.884 (15)	3.879 (9)	3.893 (6)
	3.803 (13)	3.804 (13)	3.800 (8)	3.795 (5)
	3.963 (13)	3.968 (13)	3.941 (8)	3.935 (5)
	3.922 (13)	3.908 (13)	3.934 (8)	3.929 (5)
	3.908 (17)	3.917 (18)	3.913 (11)	3.864 (7)
Mean	3.899	3.893	3.891	3.885
Er–Mo (W)	3.893 (10)	3.883 (10)	3.889 (7)	3.878 (5)
	3.856 (11)	3.844 (12)	3.854 (8)	3.902 (6)
	3.805 (11)	3.812 (11)	3.823 (8)	3.825 (5)
	3.969 (10)	3.958 (11)	3.938 (8)	3.857 (5)
	3.961 (10)	3.972 (11)	3.961 (7)	3.938 (6)
	3.878 (13)	3.869 (14)	3.838 (10)	3.859 (12)
Mean	3.894	3.889	3.884	3.877

of two coordinate bridging oxygen atoms, which leaves M–O bond lengths unchanged but decreases average angle of M–O–W while making the two cations closer, leading to the presence of NTE. It is seen from Table 4 that average distances between Y and W(Mo) decrease from 3.899 to 3.885 Å and 3.894 to 3.877 Å for $Y_2W_{2.5}Mo_{0.5}O_{12}$ and $Y_2W_{0.5}Mo_{2.5}O_{12}$, respectively. In this study, the change of NTE can be attributed to variation of bond strength. For example, substitution of Mo and W makes the bond W(Mo)–O weaker than unsubstituted bond W–O and Mo–O and the weaker bonds, in turn, decrease rigidity of WO_4. Lightfoot and Sleight et al. [4, 10] have reported that the rigidity of structure can affect the NTE property, the more rigid polyhedra are, the larger NTE the compound tends to show. Therefore, in this study the substitution of Mo and W weaken the NTE property of $Y_2W_3O_{12}$ and $Y_2Mo_3O_{12}$.

Conclusion

A novel class of solid solutions $Y_2W_{3-x}Mo_xO_{12}$ ($0.5 \leq x \leq 2.5$) were successfully prepared and characterized by Rietveld analysis of X-ray powder diffraction data. The lattice parameters do not show regular trend with

increasing Mo content. For $x = 1.5$, a mixture of two pure phases appears. Water molecule absorbed in the structure can affect cell parameters of $Y_2W_{3-x}Mo_xO_{12}$.

Negative thermal expansion properties of $Y_2W_{3-x}Mo_xO_{12}$ ($x = 0.5, 2.5$) were studied by high-temperature XRD. Substitution of Mo and W both weaken the NTE property of $Y_2W_3O_{12}$ and $Y_2Mo_3O_{12}$. It is proposed that change of W(Mo)–O bond strength affects the NTE properties through its effect on WO_4 rigidity.

References

1. Evans JSO, Mary TA, Sleight AW (1998) J Solid State Chem 137:148
2. Evans JSO, Mary TA (2000) Int J Inorg Mater 2:143
3. Forster PM, Sleight AW (1999) Int J Inorg Mater 1:123
4. Woodcock DA, Lightfoot P, Ritter C (2000) J Solid State Chem 149:92
5. Sumithra S, Umarji AM (2005) Mater Res Bull 40:167
6. Marinkovic BA, Jardim PM, de Avillez RR, Rizzo F (2005) Solid State Sci 7:1377
7. Xiao XL, Cheng YZ, Peng J, Wu MM, Chen DF, Hu ZB et al (2008) Solid State Sci 10:321
8. Sumithra S, Tyagi AK, Umarji AM (2005) Mat Sci Eng B 116:14
9. Sumithra S, Umarji AM (2006) Solid State Sci 8:1453
10. Forster PM, Yokochi A, Sleight AW (1998) J Solid State chem 140:157
11. Shannon RD (1976) Acta Cryst A32:751
12. Jia YQ (1991) J Solid State Chem 95:184
13. Sumithra S, Umarji AM (2004) Solid State Sci 6:1313
14. Zhao XH (1999) Chem J Chinese U 20:339
15. Shen R, Wang TM (2004) Rare Metal Mat Eng 33:91
16. Rodriguez-Carvajal J (2005) Program Fullprof.2k, version 3.30, Laboratoire Leon Brillouin, France
17. Lubarda VA (2003) Mech Mater 35:53
18. Lambregts MJ, Frank S (2004) Talanta 62:627
19. Duan N, Kameswari U, Sleight AW (1999) J Am Chem Soc 121:10432
20. Xing XR, Chen J, Deng JX, Liu GR (2003) J Alloys Compd 360:286